

Article

Development and Application of an Electrochemical Sensor with 1,10-Phenanthroline-5,6-dione-Modified Electrode for the Detection of *Escherichia coli* in Water

Yining Fan ^{1,2,†}, Yanran Liu ^{1,2,†}, Guanyue Gao ^{1,2,*} , Hanxin Zhang ^{1,2} and Jinfang Zhi ^{1,2}

¹ Key Laboratory of Photochemical Conversion and Optoelectronic Materials, Technical Institute of Physics and Chemistry, Chinese Academy of Sciences, Beijing 100190, China; zhi-mail@mail.ipc.ac.cn (J.Z.)

² University of Chinese Academy of Sciences, Beijing 100049, China

* Correspondence: gaoguan Yue@mail.ipc.ac.cn

† These authors contributed equally to this work.

Abstract: The routine monitoring of bacterial populations is crucial for ensuring water quality and safeguarding public health. Thus, an electrochemical sensor based on a 1,10-phenanthroline-5,6-dione-modified electrode was developed and explored for the detection of *E. coli*. The modified electrode exhibited enhanced NADH oxidation ability at a low potential of 0.1 V, which effectively eliminated the interference from other redox compounds in bacteria. The sensitivity for NADH was 0.222 $\mu\text{A}/\mu\text{M}$, and the limit of detection was 0.0357 μM . Upon cell lysis, the intracellular NADH was released, and the concentration of *E. coli* was determined through establishing the relationship between the oxidation current signal and NADH concentration. The performance of the electrochemical sensor in the detection of NADH and *E. coli* suspensions was validated using the WST-8 colorimetric method. The blank recovery experiment in real water samples exhibited good accuracy, with recovery rates ranging from 89.12% to 93.26% and relative standard deviations of less than 10%. The proposed electrochemical sensor realized the detection of *E. coli* without the usage of biomarkers, which provides a promising approach for the broad-spectrum detection of microbial contents in complex water environments.

Keywords: electrochemical sensor; 1,10-phenanthroline-5,6-dione; NADH; *Escherichia coli*; rapid detection



Citation: Fan, Y.; Liu, Y.; Gao, G.; Zhang, H.; Zhi, J. Development and Application of an Electrochemical Sensor with 1,10-Phenanthroline-5,6-dione-Modified Electrode for the Detection of *Escherichia coli* in Water. *Chemosensors* **2023**, *11*, 458. <https://doi.org/10.3390/chemosensors11080458>

Academic Editor: Marcello Mascini

Received: 29 June 2023

Revised: 4 August 2023

Accepted: 10 August 2023

Published: 15 August 2023



Copyright: © 2023 by the authors. Licensee MDPI, Basel, Switzerland. This article is an open access article distributed under the terms and conditions of the Creative Commons Attribution (CC BY) license (<https://creativecommons.org/licenses/by/4.0/>).

1. Introduction

Biodiverse and complex water ecosystems provide favorable environments for a wide range of microorganisms, resulting in significant microbial populations within aquatic environments. However, the spreading of pathogenic microorganisms through water can lead to severe epidemics and infectious diseases [1]. Consequently, strict regulations have been established to restrict the microbial contents in various water sources, such as drinking water, surface water, and groundwater, in order to safeguard public health [2]. Recent advancements in water quality assessment methodologies have contributed to the progressive refinement of the standards concerning microbial indicators. The key microbiological indicators utilized in evaluating water quality predominantly include the total number of colonies, coliform groups, fecal coliform groups, and other pathogenic bacteria. The water standards have adopted analytical methods like flat colony counting, multitube fermentation, filter membrane, and turbidimetric counting to assessing microbial contents through enumerating colonies or measuring optical density [3]. However, these traditional culture methods require specific culture media; precise control over experimental conditions such as temperature, pH, and oxygen levels; as well as specialized instruments and skilled personnel. Additionally, their lengthy culture times and poor anti-interference ability have further limited their application in real detection scenarios. Furthermore, with the development of immunoassay and bioassay technologies, bioanalytical techniques, represented by

enzyme-linked immunosorbent assay (ELISA) and polymerase chain reaction (PCR), have offered sensitive approaches for bacterial detection with high accuracy and specificity [4]. Nevertheless, their application is constrained by their high cost and inability to meet the rapid detection requirements for multiple targets in water.

In addition to conventional standard methods, optical techniques, including fluorescence analysis [5], surface plasmon resonance [6,7], surface-enhanced Raman scattering [8,9], and electrochemical sensing, can selectively identify and sensitively detect microorganisms through the assistance of endogenous biomarkers such as antibodies/antigens, aptamers, DNA, etc. Among them, electrochemical biosensors have emerged as a promising candidate due to their fast response, ease of miniaturization, and cost-effectiveness [10–12]. Via incorporation with biomarkers, the electrochemical biosensors have achieved the sensitive detection of DNA [13], toxins [14], cancer cells [15], and bacteria [16]. Ju et al. developed a sensitive and specific electrochemical biosensor based on target-induced aptamer displacement and achieved the direct detection of *E. coli* O111 with a limit of detection (LOD) of 112 CFU/mL [16]. Güner et al. developed an electrochemical immunosensor by modifying a poly-pyrrole/Au/MWCNT/chitosan modified electrode with *E. coli* monoclonal antibodies [17]. Zou et al. employed a “sandwich” mode to capture *E. coli* with antibodies and bind them to mediators. The resulting differential pulse voltammetry signal was proportional to the number of *E. coli*, enabling an LOD of 10 CFU/mL [18]. In recent years, innovative immunosignal amplification strategies, including 3D walkers, clustered regularly interspaced short palindromic repeats (CRISPR) technology [19,20], and ring-mediated isothermal amplification, have been integrated into the development of electrochemical sensors. Zhang et al. employed a 3D DNA walking molecule amplification strategy in the detection of *E. coli*, achieving an LOD of 20 CFU/mL [21].

Electrochemical sensors can also achieve indirect bacterial detection through the detection of intracellular endogenous substances. Kwon et al. detected the reduction current of 4-methoxyphenyl- β -D-galactopyranoside to 4-methoxyphenol under the catalysis of the β -galactosidase present in *E. coli* and realized the detection of *E. coli* with an LOD of 2×10^3 CFU/mL [22]. Currently, most electrochemical biosensors rely on bio-immune and DNA analysis, which possess high specificity [23–25], but this characteristic also leads to constraints in the detection of multiple microorganisms. The use of nonbiological identification methods to achieve broad-spectrum detection of microorganisms is still relatively rare.

In present study, an electrochemical sensor was fabricated using 1,10-phenanthroline-5,6-dione as a redox mediator, and its potential for quantitatively detecting NADH and *E. coli* was investigated. The performance and anti-interference ability of the as-prepared electrochemical sensor were evaluated. To determine the accuracy of the electrochemical sensor in quantifying *E. coli* concentration and intracellular NADH content, a WST-8 colorimetric method was employed. Additionally, three real river water samples were collected, and a blank recovery experiment was conducted to assess the capability of the electrochemical sensor in detecting *E. coli* concentrations. The primary objective of this work was to determine the *E. coli* population using NADH as a signal indicator, thereby creating a feasible and broad-spectrum method for the detection of microorganisms in complex water samples.

2. Materials and Methods

2.1. Reagents

Escherichia coli (ATCC 25922) was provided by China General Microbiological Culture Collection Center. The 1,10-phenanthroline-5,6-dione (PD), nicotinamide adenine dinucleotide (NADH), thionine (TH), reduced flavin adenine dinucleotide (FADH₂), agar, tri (hydroxymethyl) amino methane hydrochloride (Tris-HCl), and ethylene diamine tetraacetic acid (EDTA) were all purchased from Beijing Lanyi Chemical Products Co., Ltd., Beijing, China. Multiwalled carbon nanotubes (MWCNTs) were provided by XFNANO Co., Ltd., Nanjing, China. Triton X-100 and NAD⁺/NADH assay kits were purchased from Beyotime

Biotechnology Co., Ltd., Shanghai, China. We purchased 0.1 M phosphate buffer solution (PBS) from Sinopharm Chemical Reagent Co., Ltd., Shanghai, China, and 5% Nafion™ 117 solution was purchased from Merck, Darmstadt, Germany. Beef extract and peptone were purchased from Aoboxing biotech company, Beijing, China. All chemicals were used without further purification. Milli-Q water ($R > 18.0 \text{ M}\Omega\bullet\text{cm}$) was used to prepare all solutions.

Three real water samples were collected from Puhe River in Shanxi Province, Tangwang River in Heilongjiang Province, and Xiaoyun River in Beijing. All the real water samples were filtered through a $13 \text{ mm} \times 0.22 \mu\text{m}$ filtration membrane to remove the sediments before electrochemical detection.

2.2. Apparatus

Cyclic voltammetry (CV) and chronoamperometric measurements were carried out with an electrochemical workstation (CHI 660E). Field-emission scanning electron microscopy (FESEM, Quanta FEG 250, Oregon, OR, USA) with an operating voltage of 10 kV was used to characterize the morphology of the modified electrode. The concentration of *E. coli* in the suspension was measured with a UV spectrophotometer (SECOMAM UVIKONXL, Domont, France) at 600 nm, recorded as OD_{600} . OD_{600} refers to the light absorption value of a bacterial solution at a wavelength of 600 nm, which is used to characterize bacterial concentrations. The higher the bacterial concentration, the higher the absorbance [26,27].

2.3. Preparation of Electrochemical Sensor

We dissolved 100 mg of MWCNTs in 10 mL of deionized water, which we then dispersed ultrasonically for 30 min. Then, 100 μL of 5% Nafion solution was added and mixed ultrasonically for 5 min to prepare the MWCNTs–Nafion solution. We dropped 15 μL of as-prepared MWCNTs–Nafion solution on the surface of a glassy carbon electrode (GCE), which was dried at room temperature to form MWCNTs–Nafion@GCE. Then, 5 mg of PD was dissolved in 5 mL ethanol solution and sonicated for 10 min to prepare PD solution; 10 μL of PD solution was dropped on the MWCNTs–Nafion@GCE and dried for 2 h. The modified electrode was rinsed with deionized water and dried at room temperature to obtain PD–MWCNTs–Nafion@GCE, which was stored in a refrigerator at 4 °C until use.

Similarly, the TH-modified electrode was prepared according to same procedure. A total of 10 μL of 0.3 mM TH aqueous solution was dropped on MWCNTs–Nafion@GCE and dried for 2 h. Then, the modified electrode was rinsed with deionized water to remove excess TH and dried at room temperature to obtain TH–MWCNTs–Nafion@GCE.

2.4. Culture of *E. coli*

A small aliquot of *E. coli* was placed in 100 mL of liquid culture medium that contained 5 g/L beef extract, 10 g/L peptone, and 5 g/L sodium chloride. Then, the inoculated culture medium was cultured aerobically in a rotary shaker in a 37 °C water bath for 16 h. The cultured bacterial suspension was centrifuged at 6000 rpm for 5 min and washed twice with PBS solution to fully remove the culture medium. The concentration of *E. coli* suspension was adjusted using a UV spectrophotometer and diluted to different concentrations ranging from $\text{OD}_{600} = 0.2$ to $\text{OD}_{600} = 2.6$.

The number of *E. coli* in bacterial suspension with varied OD_{600} values was further determined using the flat colony counting method. Solid agar culture plates were prepared as follows: The agar liquid medium (beef extract 5 g/L, peptone 10 g/L, sodium chloride 5 g/L, and agar 15 g/L) was first fully mixed and sterilized at 121 °C. The liquid agar medium was then cooled to 46 °C and poured into the plates and solidified at room temperature. *E. coli* suspensions with different OD_{600} values were fully diluted, then 1 mL of dilution was dropped into the sterile agar plate and cultured at 37 °C for 24 h. Three parallel groups were set for each OD_{600} value. The number of *E. coli* colonies was observed

and counted with a colony counter, and the bacterial concentration in each OD₆₀₀ value is presented as colony-forming units per milliliter (CFU/mL).

2.5. Detection of NADH Using As-Prepared Electrochemical Sensor

A three-electrode electrochemical cell was used to determine the content of NADH. The as-prepared PD-MWCNTs-Nafion@GCE was used as the working electrode, a Pt wire was used as the counter electrode, and Ag/AgCl (sat' KCl) was used as the reference electrode. During the detection process, the modified electrode was initially activated in 10 mL of 0.1 M PBS solution (pH = 7.0) under 900 rpm stirring. The applied potential was 0.1 V vs. Ag/AgCl (sat' KCl). Standard NADH solutions with varied concentrations were added into the electrochemical cell once the current was steady, and the current values were measured 30 s after each addition. The calibration curve was obtained by plotting the current changes (ΔI) against the corresponding NADH concentrations.

2.6. Detection of *E. coli* Using As-Prepared Electrochemical Sensor

The *E. coli* concentration was determined by quantitatively analyzing their intercellular NADH content. Therefore, cells lysis was conducted to release the intracellular NADH in order to detect *E. coli* concentration. We mixed 5 mL of *E. coli* suspension with different OD₆₀₀ values with 0.1 M Tris-HCl, 0.02 M EDTA, and 0.05% Triton X-100, and sonicated in an ice bath for 15 min to prepare *E. coli* lysate.

The concentration of *E. coli* was determined via chronoamperometry. The current response of the as-prepared PD-MWCNTs-Nafion@GCE in 10 mL of *E. coli* lysate was recorded at the applied potential of 0.1 V. The steady-state current was recorded after 100 s, and the current–concentration relationship was established by detecting *E. coli* suspension with various OD₆₀₀ values.

2.7. Detection of *E. coli* Using Colorimetric Method

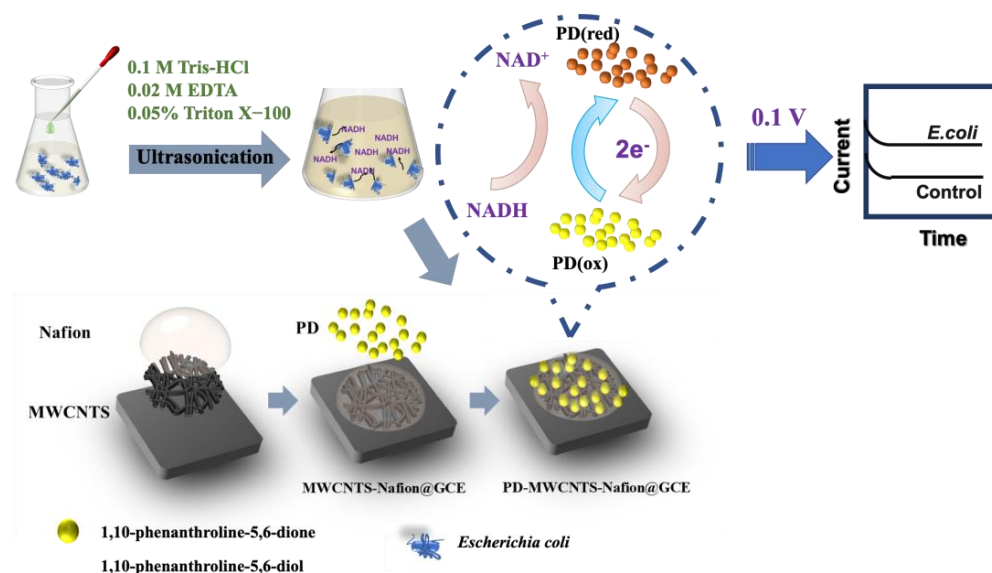
The intracellular concentration of NADH was also verified using the WST-8 colorimetric method with the following procedure: We prepared 20 μ L of 0, 0.25, 0.5, 1, 2, 4, 6, 8, and 10 μ M standard NADH solutions, which we added into a 96-well plate. Then, 20 μ L of *E. coli* lysate with varying OD₆₀₀ values was also added into the 96-well plate for detection. Next, 90 μ L of PBS and 10 μ L of 1-methoxy-5-methylphenazinium methyl sulfate chromogenic solution were added into each sample, which were then incubated in the dark for 45 min. The absorbance intensity was measured at a wavelength of 450 nm with a microplate reader (TECAN Infinite50, Männedorf, Switzerland). According to the established absorbance intensity–NADH concentration calibration curve, the NADH concentrations in *E. coli* lysate were determined.

3. Results and Discussion

3.1. The Detection Principles of As-Prepared Electrochemical Sensor

In this work, a novel electrochemical approach was developed for the sensitive detection of *E. coli* based on the quantification of intracellular NADH content. NADH is a crucial product of microbial carbohydrate metabolism and plays a vital role in the microbial respiratory electron transfer processes. Studies have demonstrated that the number of NADH molecules within each bacterial cell remains relatively constant, typically ranging from 10⁶ to 10⁸, making NADH a stable and universally present endogenous substance in bacterial systems [28]. However, it is important to identify the specific potential at which NADH can undergo oxidation to coenzyme I in the electrochemical detection of NADH. This oxidation process typically occurs at high oxidation potentials, resulting in the concurrent oxidation of other intracellular electroactive substances and subsequently the generation of interference signals. Nevertheless, previous research has indicated that PD is an ideal mediator capable of oxidizing NADH at a lower potential, thus enabling selective and accurate detection [29].

In the design of electrochemical sensors, MWCNTs are widely employed as electrode-modification materials, which exhibit remarkable electrochemical stability and electrical conductivity [30]. Nafion, as a type of perfluorosulfonic acid polymer, exhibits good thermal stability and high proton conductivity. It has been revealed that the interaction between the hydrophobic sidewalls of MWCNTs and the main chain of Nafion fluorocarbons facilitates the uniform dispersion of MWCNTs within Nafion, effectively enhancing Nafion's ability to immobilize MWCNTs on the electrode [31]. Consequently, the integration of these materials can enhance electrode conductivity while simultaneously improving the immobilization of the PD mediator on the electrode surface. Therefore, we developed a PD-mediated electrochemical sensor to detect NADH at low potential, subsequently realizing the accurate quantification of *E. coli* concentrations. The electrode preparation and *E. coli* detection process are depicted in Scheme 1. The GCE was first modified with MWCNTs–Nafion solution to form a polymer film. Then, PD mediator was drop casted on the MWCNTs–Nafion@GCE, and the PD-modified electrode was prepared. In the *E. coli* detection process, the bacterial suspension was incubated with cell lysis buffer to fully release the intracellular NADH. The NADH content was determined using the as-prepared PD-modified electrode at a suitable potential, and the current response was recorded.



Scheme 1. Schematic representation of the preparation and detection process of electrochemical sensor.

3.2. Surface Characterization of PD-Modified Electrode

The morphologies of the PD particles, MWCNTs, and modified electrodes were characterized using a field-emission scanning electron microscope, the results are shown in Figure 1. Needle-like clusters of PD particles with different shapes and sizes were observed, indicating the agglomeration of PD particles on the GCE surface (Figure 1a). The morphology of the MWCNTs is shown in Figure 1b, which had an average tube length of 8 μm . The as-prepared PD-MWCNTs-Nafion@GCE was uniformly covered by a smooth and porous film, signifying the successful deposition of the Nafion film onto the GCE (Figure 1c). The presence of large particles on the electrode surface corresponded to agglomerated PD, while the tubular structures indicated that the MWCNTs were partially embedded within the Nafion film. The above results demonstrated the effective immobilization of both PD and MWCNTs on the electrode surface through Nafion.

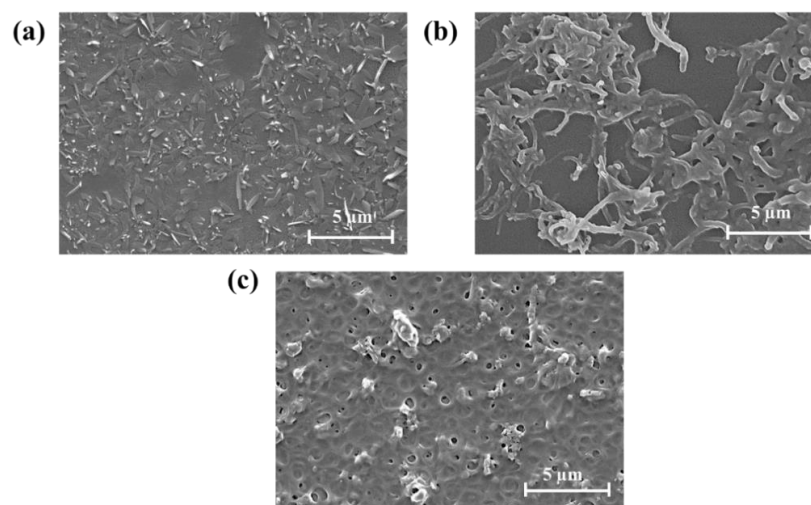


Figure 1. FESEM images of different modified electrodes: (a) PD@GCE; (b) MWCNTs@GCE; (c) PD-MWCNTs-Nafion@GCE.

3.3. Electrochemical Characterization of PD-Modified Electrode

The electrochemical properties of the modified electrodes were firstly examined via cyclic voltammetry, as shown in Figure 2a. In PBS solution, PD-MWCNTs-Nafion@GCE exhibited oxidation and reduction peaks at 0.05 V and -0.13 V (Figure 2a, red dashed line), representing the oxidation and reduction of PD mediator. Notably, the PD-modified electrode displayed good reversibility with a ΔE_p value of 0.18 V. In the absence of the PD mediator, no redox peak was observed for MWCNTs-Nafion@GCE, owing to the inherent stability of MWCNTs and Nafion polymer (Figure 2a, blue dashed line).

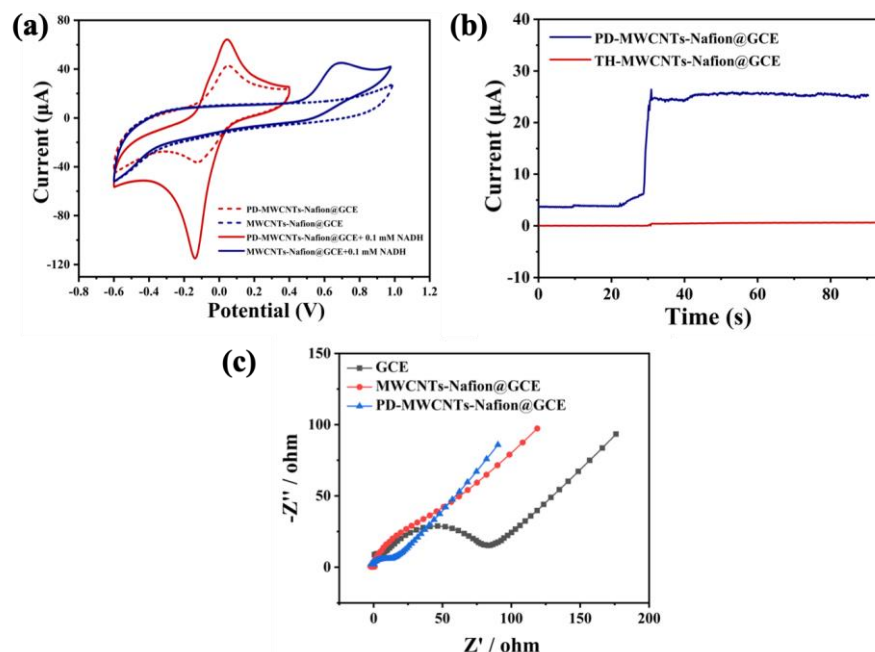
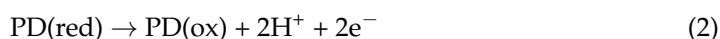
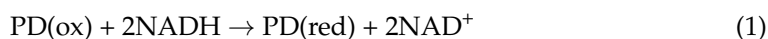


Figure 2. (a) Cyclic voltammograms of PD-MWCNTs-Nafion@GCE and MWCNTs-Nafion@GCE before and after the addition of 0.1 mM NADH, scan rate 0.1 V/s; (b) $i-t$ curves of TH-MWCNTs-Nafion@GCE and PD-MWCNTs-Nafion@GCE in 0.1 mM NADH at a potential of 0.1 V (vs. Ag/AgCl); (c) Nyquist plots of bare GCE and modified electrodes.

Moreover, the electrochemical reaction between the modified electrode and NADH was also investigated. In 0.1 mM NADH solution, the MWCNTs-Nafion@GCE electrode displayed a distinct oxidation peak at approximately 0.6 V (Figure 2a, blue line), indicating

that NADH undergoes oxidation and decomposition at a high potential on MWCNTs-Nafion@GCE. It is worth noting that many substances, such as uric acid and ascorbic acid, can also undergo direct oxidation at a potential of 0.6 V. Hence, NADH detection at this potential suffers from poor anti-interference ability. In contrast, the PD-MWCNTs-Nafion@GCE exhibited a much more sensitive response to NADH (Figure 2a, red line). The oxidation of NADH was achieved at a much lower potential of 0.05 V, and the oxidation peak current of the modified electrode increased by 20 μA after 0.1 mM NADH addition. This decrease in oxidation potential offers several advantages: On the one hand, the decrease in oxidation potential can effectively avoid the electrode fouling caused by high potential oxidation and the signal interference caused by the oxidation reactions of other substances in water samples. On the other hand, the enhanced redox signal response can further improve the sensitivity in NADH and *E. coli* detection. This improved performance of the PD-MWCNTs-Nafion@GCE electrode can be attributed to the reactions between the PD mediator and NADH. As shown in Equations (1) and (2), PD catalyzes the oxidative decomposition of NADH and is reduced to 1,10-phenanthroline-5,6-diol; then, 1,10-phenanthroline-5,6-diol is oxidized back to PD under the applied oxidation potential and generates an oxidation current.



In order to verify the superiority of PD as a mediator in the detection of NADH, we also considered the electrochemical performance of a thionine-modified electrode. TH is a widely used mediator in the construction of microbial biosensors and microbial fuel cells, which possesses good electron transfer ability in bacterial metabolic processes [32]. The chronoamperometric responses of modified electrodes utilizing different mediators were assessed in the detection of NADH. As depicted in Figure 2b, the TH-modified electrode only exhibited a feeble oxidation current ($\Delta I = 0.5 \mu\text{A}$) upon the addition of 0.1 mM NADH (Figure 2b, red line). In comparison, the PD-modified electrode demonstrated a distinct current response ($\Delta I = 21.6 \mu\text{A}$, Figure 2b, blue line) because TH reacts with NADH at a negative potential, which leads to the low oxidation efficiency at 0.1 V. Therefore, PD is a more favorable mediator in the detection of NADH at low potentials.

The changes in the modified electrode's interfacial properties were characterized using electrochemical impedance spectroscopy (EIS). The impedance spectra of different electrodes were recorded in 0.1 M KCl solution containing 5.0 mM $[\text{Fe}(\text{CN})_6]^{3-}/[\text{Fe}(\text{CN})_6]^{4-}$ at a frequency ranging from 10^5 to 10^{-1} Hz. As depicted in Figure 2c, the Nyquist plot of bare GCE appears as an oblique line at low frequencies and a semicircle at high frequencies, with an R_{ct} of 90 Ω . After the modification of MWCNTs-Nafion, the R_{ct} value remained at the same level. It could be attributed to the combined effect of the high conductivity of carbon nanotubes and the electrostatic repulsion of Nafion membranes against $[\text{Fe}(\text{CN})_6]^{3-}/[\text{Fe}(\text{CN})_6]^{4-}$ mediators. Notably, the R_{ct} value decreased to 15 Ω after the adsorption of PD, which demonstrated the effect of the PD mediator in facilitating the electron transfer process of PD-MWCNTs-Nafion@GCE.

3.4. The Performance of As-Prepared Electrochemical Sensor in NADH Detection

To validate the feasibility of as-prepared electrochemical sensor in the detection of NADH, chronoamperometric measurements were performed by consecutively adding NADH at varying concentration gradients. As shown in Figure 3a, when 10 μM NADH was added, the diffusion equilibrium was reached within 10 s under stirring, and the steady-state current was obtained. The current change–NADH concentration relationships between 10–100 μM and 0.25–8 μM were established according to the amperometric results. As shown in Figure 3b, the as-prepared electrochemical sensor exhibited excellent linear relationships in both the higher and lower concentration ranges. The correlation coefficients were above 0.99, indicating high accuracy in NADH detection. The sensitivity for NADH

was $0.222 \mu\text{A}/\mu\text{M}$, and the LOD value was $0.0357 \mu\text{M}$. The LOD was calculated using $3 S_b/m$, where m is the slope of calibration curve at low concentration, and S_b is standard deviation from three blank experiments. Compared with previously reported sensors (Table 1), the present electrochemical sensor has a relatively low detection limit. In addition, our method could be operated at a relatively low voltage, which can effectively prevent interference from other electroactive substances.

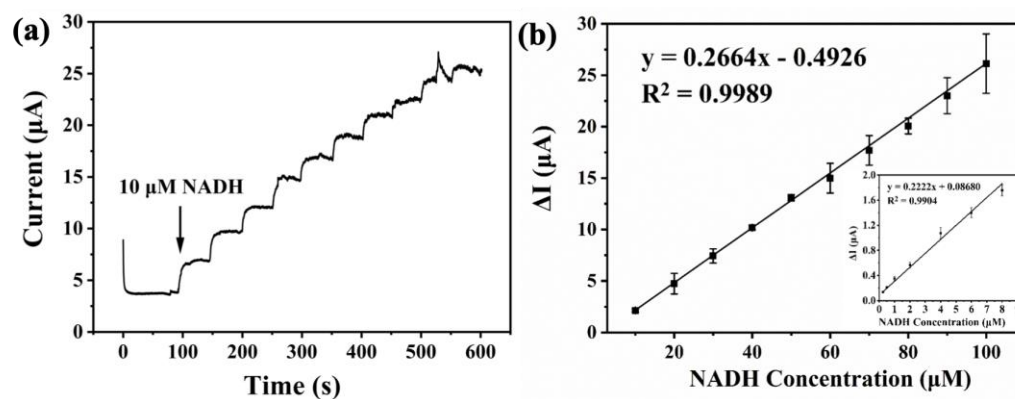


Figure 3. (a) *i*-*t* curves of PD-MWCNTs-Nafion@GCE in the detection of NADH, $E = 0.1 \text{ V}$ (vs. Ag/AgCl); (b) calibration curves for NADH.

Table 1. Comparison of electrochemical sensors in the detection of NADH.

Sensor	Detection Potential (V)	LOD (μM)	Linear Range (μM)	Sensitivity ($\mu\text{A}/\mu\text{M}$)	Ref.
CS-DA-MWCNTs-COOH/Au	+0.25 vs. SCE	0.012	0.1–600	0.009	[33]
PAA-MWNTs/GCE	+0.13 vs. Ag/AgCl	1	4–100	0.094	[34]
ERGO-PTH/GC	+0.4 vs. SCE	0.1	10–3900	0.143	[35]
CHIT/MWNTs/GC	+0.4 vs. SCE	0.3	0.8–1600	/	[36]
POA/GR@GCE	+0.045 vs. SCE	1.3	0.166–1.772	47.1	[37]
PD-MWCNTs-Nafion@GCE	+0.1 vs. Ag/AgCl	0.0357	0.25–8, 10–100	0.222	This work

The bacterial respiratory metabolism is a complex process involving cytochrome *c*, cytochrome *a*, FADH_2 , and various enzymes involved in respiratory electron transfer, such as NADH dehydrogenase, coenzyme Q, succinate dehydrogenase, etc. Thus, the anti-interference experiment was conducted to evaluate the potential impact of active intracellular redox substances on the oxidation current signal of NADH. Among these substances, coenzyme Q exhibited an anodic peak at approximately -0.1 V and cytochrome *c* at -0.26 V for MWCNTs-modified GCE [38,39], which do not interfere with the NADH oxidation signal. In contrast, FADH_2 , which participates in the ATP conversion process together with NADH, is an electron donor similar to NADH, which may potentially interfere with the oxidation of NADH. Therefore, an interference experiment was conducted to examine whether FADH_2 generates an oxidation current under the same experimental conditions. A potential of 0.1 V was applied on the modified electrode, and chronoamperometry was performed in 0.1 M PBS solution. The result is shown in Figure 4a: no significant current increase was observed after the addition of 0.1 mM FADH_2 , indicating that FADH_2 does not interfere with the redox reaction of PD and NADH at a potential of 0.1 V . This result was also verified via the cyclic voltammetry of PD-MWCNTs-Nafion@GCE in the presence of FADH_2 . The CV curve displayed distinct redox peaks for FADH_2 at -0.3 V and -0.5 V , respectively, which suggested the low redox potential of FADH_2 on the modified electrode (Figure 4b). The PD mediator was not involved in the oxidation of FADH_2 at a potential of 0.1 V . Therefore, the electrochemical sensor showed nonresponse to FADH_2 during the detection process. In summary, the low oxidation potential of PD and NADH effectively eliminates the interference of active intracellular redox substances during the detection

process, ensuring the specificity and accuracy of the as-prepared electrochemical sensor in the detection of NADH.

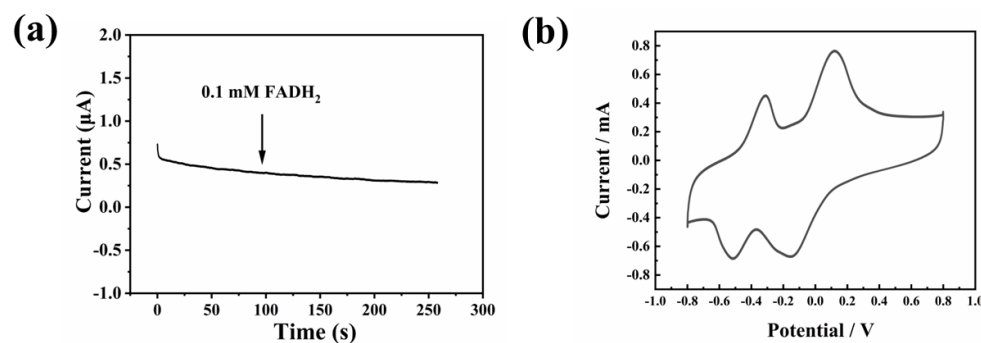


Figure 4. (a) *i*-*t* curve of PD-MWCNTs-Nafion@GCE upon the addition of 0.1 mM FADH₂ (in 0.1 M PBS), *E* = 0.1 V (vs. Ag/AgCl). (b) Cyclic voltammetry of PD-MWCNTs-Nafion@GCE in 0.1 M PBS solution containing FADH₂ at the scan rate of 0.1 V/s.

3.5. Detection of *E. coli* by As-Prepared Electrochemical Sensor

In water quality assessments, the amount of *E. coli* and the total number of bacterial colonies are crucial microbial parameters. Therefore, the applicability of the as-prepared electrochemical sensor in detecting *E. coli* was investigated. Chronoamperometry was employed to detect *E. coli* lysates with varying concentrations. The chronoamperometric response of the electrochemical sensor to *E. coli* lysates with OD₆₀₀ values of 0, 0.4, 0.77, 1.2, 1.64, and 2.0 is shown in Figure 5a. The steady-state currents increased with rising concentrations of *E. coli* suspension. The steady-state current of the *E. coli* suspension with OD₆₀₀ values of 0.4 and 0.77 were 0.32 µA and 0.37 µA, respectively, while the steady-state current of OD₆₀₀ = 2.0 reached 1.53 µA. It is worth noting that the relationship between the current response and OD₆₀₀ values was found to be nonlinear. In order to explore the underlying reason for this phenomenon, the numbers of *E. coli* colonies under different OD₆₀₀ values from 0.2 to 2.6 were detected using the plate colony counting method. The relationship of the current response and *E. coli* colony numbers is illustrated in Figure 5b; the current-*E. coli* colony numbers conformed to a linear relationship at low bacterial concentrations, which indicated that the NADH concentrations in bacterial lysates increased linearly with *E. coli* colony numbers. However, the current response slowly plateaued as *E. coli* colony numbers further increased. This could be attributed to the insufficient cell lysis and nonexhaustive release of intracellular NADH as the bacterial content further increased. The LOD of the as-prepared electrochemical sensor for *E. coli* was determined using $3S_b/m$, where *m* is the slope at low concentrations, and *S_b* is the standard deviation for three blank measurements. The LOD value for *E. coli* was 1.12×10^{10} CFU/mL. Therefore, the as-prepared sensor can accurately detect the NADH content in *E. coli* solutions, and the detection signal is positively correlated with the *E. coli* concentration, which further proves the suitability of the electrochemical sensor for the detection of *E. coli*.

To further validate the accuracy of the as-prepared electrochemical sensor in the quantification of NADH content in *E. coli* solutions, three *E. coli* lysate samples with OD₆₀₀ values of 0.2, 1.0, and 1.5 were selected for analysis. The NADH concentrations in these bacterial lysates were determined with both the electrochemical sensor and the WST-8 colorimetric method. To determine the NADH concentration in unknown samples via the WST-8 colorimetric method, the calibration curve between absorbance intensity and NADH concentration was established. As shown in Figure 6a, the absorbance intensity and NADH concentration conformed to a good linear relationship. Subsequently, the NADH contents of *E. coli* lysates with OD₆₀₀ values of 0.2, 1.0, and 1.5 were detected following the same procedure. To eliminate solution turbidity from interfering with the absorbance intensity, the supernatants of the *E. coli* lysates were obtained through centrifugation. By comparing the detected absorbance intensity values with the calibration curve, the NADH

concentrations in *E. coli* lysates were determined to be 0.965 μM , 2.194 μM , and 5.429 μM for OD_{600} values of 0.2, 1.0, and 1.5, respectively.

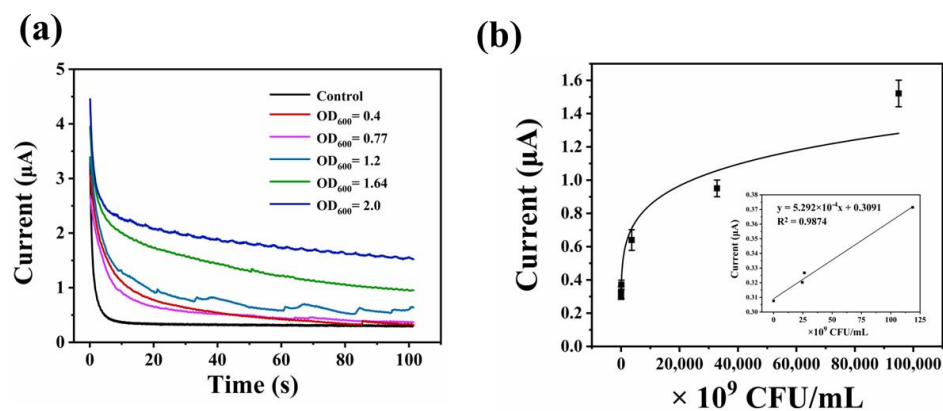


Figure 5. (a) *i*-*t* curves of as-prepared electrochemical sensor in the detection of *E. coli* in solution with different OD_{600} values, $E = 0.1$ V (vs. Ag/AgCl); (b) relationship of current response with *E. coli* colony numbers.

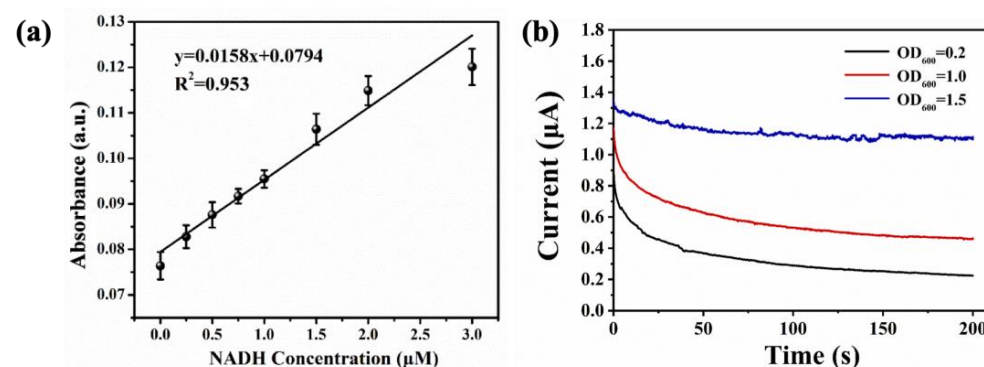


Figure 6. (a) Linear curve of NADH concentration and absorbance intensity obtained with WST-8 colorimetric method; (b) *i*-*t* curves of as-prepared electrochemical sensor in the detection of *E. coli* solution with different OD_{600} values, $E = 0.1$ V (vs. Ag/AgCl).

The NADH contents of the aforementioned *E. coli* lysate samples were also assessed using the electrochemical sensor. As depicted in Figure 6b, the ΔI observed for the three *E. coli* lysates with OD_{600} values of 0.2, 1.0, and 1.5 were 0.221 μA , 0.452 μA , and 1.110 μA , respectively. By comparing these current responses to the established current–NADH concentration relationship (Figure 3b), the NADH concentrations were determined to be 1.008 μM , 2.120 μM , and 5.294 μM , respectively. The relative standard deviations (RSDs) between these two methods were 4.46%, 3.37%, and 2.48%. These results demonstrated that the proposed electrochemical sensor has excellent accuracy in NADH detection when compared with the WST-8 colorimetric method.

3.6. *E. coli* Detection in Real Water Samples

The applicability of the electrochemical sensor in detecting *E. coli* concentrations in real water was evaluated through a blank recovery experiment. Three real water samples were collected from cities, villages, and rural regions across different provinces. To eliminate the interference by intrinsic microorganisms, we employed the WST-8 technique to determine the NADH concentration in the real water samples. The result indicated that the NADH concentrations were lower than the detection limit. Hence, the contents of native microbes in the real water samples were extremely low and could be disregarded. Therefore, a blank recovery experiment was performed to investigate the feasibility of the developed electrochemical sensor for *E. coli* detection with real water samples. The same amount

of *E. coli* suspension with $OD_{600} = 0.2$ was added into these real water samples, and the current responses and colorimetric changes were recorded. The NADH concentration in the *E. coli* suspension was determined to be $0.0965 \mu\text{M}$ using the WST-8 colorimetric method. The detected NADH concentrations and recovery rates of the three water samples determined with electrochemical sensor are listed in Table 2. The recovery rates of the NADH concentrations detected with the electrochemical sensors ranged from 89.12% to 93.26%. The RSD values between two method were less than 10%. The standard deviation for the as-prepared electrochemical sensor was $0.002 \mu\text{M}$. These results confirm the good accuracy of the electrochemical sensor in quantifying NADH contents, thereby demonstrating the capability of the electrochemical sensor based on a PD mediator to detect the number of *E. coli* colonies in real water.

Table 2. Results of NADH blank recovery tests in three water samples.

Water Sample	NADH Concentration Detected with Electrochemical Sensor (μM)	Recovery Rate (%)	RSD (%)
Pu River	0.086	89.12	8.26
Tangwang River	0.090	93.26	2.08
Xueqing River	0.088	91.19	4.45

4. Conclusions

In this study, we successfully developed an electrochemical sensor utilizing 1,10-phenanthroline-5,6-dione as a mediator, which demonstrated good capabilities in both NADH detection and *E. coli* determination. The experimental results demonstrated that the utilization of the PD mediator significantly reduced the applied potential, leading to improved anti-interference ability. There was good linear relationship between the NADH concentration and current response of the as-prepared electrochemical sensor. Furthermore, the applicability of as-prepared electrochemical sensor in bacterial detection was verified using *E. coli* as a model organism. The results of comparative analysis with the WST-8 colorimetric method revealed that the electrochemical sensor exhibited good accuracy in detecting both *E. coli* suspensions and real water samples. Even though our study only investigated the performance in the detection of *E. coli*, as NADH widely exists in various bacterial species, the as-prepared sensor may also be feasible for the detection of total colony numbers in water samples, offering a promising approach for the broad-spectrum detection of microbial contents in complex water samples without the usage of biomarkers.

Author Contributions: Conceptualization, Y.L., G.G. and J.Z.; methodology, Y.F. and Y.L.; validation, Y.F. and Y.L.; formal analysis, Y.F. and Y.L.; investigation, Y.L. and Y.F.; data curation, Y.F. and G.G.; writing—original draft preparation, Y.L., G.G., H.Z. and J.Z.; writing—review and editing, G.G. and J.Z.; visualization, Y.F.; supervision, G.G. and J.Z.; funding acquisition, G.G. and J.Z. All authors have read and agreed to the published version of the manuscript.

Funding: This research was funded by the National Key Research and Development Program, grant number 2022YFB3304003; and the Presidential Foundation of Technical Institute of Physics and Chemistry, grant number E2A8F301.

Institutional Review Board Statement: Not applicable.

Informed Consent Statement: Not applicable.

Data Availability Statement: The data are available upon request to the corresponding author.

Conflicts of Interest: The authors declare no conflict of interest.

References

- Guo, X.D.; Han, J.Z.; Li, J.Y.; Wang, Z.B.; Zhang, Z.H.; Kang, X.; Zhu, W.; Deng, H.B. Water hazard detection: A 20-year review. *J. Terramechanics* **2023**, *105*, 53–66. [\[CrossRef\]](#)
- Ribeiro, V.H.A.; Moritz, S.; Rehbach, F.; Reynoso-Meza, G. A novel dynamic multi-criteria ensemble selection mechanism applied to drinking water quality anomaly detection. *Sci. Total Environ.* **2020**, *749*, 142368. [\[CrossRef\]](#)

3. Zulkifli, S.N.; Rahim, H.A.; Lau, W.J. Detection of contaminants in water supply: A review on state-of-the-art monitoring technologies and their applications. *Sens. Actuators B Chem.* **2018**, *255*, 2657–2689. [[CrossRef](#)] [[PubMed](#)]
4. Nnachi, R.C.; Sui, N.; Ke, B.W.; Luo, Z.H.; Bhalla, N.; He, D.P.; Yang, Z.G. Biosensors for rapid detection of bacterial pathogens in water, food and environment. *Environ. Int.* **2022**, *166*, 107357. [[CrossRef](#)] [[PubMed](#)]
5. Huang, Y.R.; Chen, W.J.; Chung, J.; Yin, J.; Yoon, J. Recent progress in fluorescent probes for bacteria. *Chem. Soc. Rev.* **2021**, *50*, 7725–7744. [[CrossRef](#)]
6. Syal, K.; Iriya, R.; Yang, Y.Z.; Yu, H.; Wang, S.P.; Haydel, S.E.; Chen, H.Y.; Tao, N.J. Antimicrobial Susceptibility Test with Plasmonic Imaging and Tracking of Single Bacterial Motions on Nanometer Scale. *ACS Nano* **2016**, *10*, 845–852. [[CrossRef](#)]
7. Li, Y.S.; Zhu, J.W.; Zhang, H.Y.; Liu, W.M.; Ge, J.C.; Wu, J.S.; Wang, P.F. High sensitivity gram-negative bacteria biosensor based on a small-molecule modified surface plasmon resonance chip studied using a laser scanning confocal imaging-surface plasmon resonance system. *Sens. Actuators B Chem.* **2018**, *259*, 492–497. [[CrossRef](#)]
8. Andrei, C.C.; Moraillon, A.; Lau, S.; Felidj, N.; Yamakawa, N.; Bouckaert, J.; Larquet, E.; Boukherroub, R.; Ozanam, F.; Szunerits, S.; et al. Rapid and sensitive identification of uropathogenic *Escherichia coli* using a surface-enhanced-Raman-scattering-based biochip. *Talanta* **2020**, *219*, 121174. [[CrossRef](#)]
9. Tadesse, L.F.; Ho, C.S.; Chen, D.H.; Arami, H.; Banaei, N.; Gambhir, S.S.; Jeffrey, S.S.; Saleh, A.A.E.; Dionne, J. Plasmonic and Electrostatic Interactions Enable Uniformly Enhanced Liquid Bacterial Surface-Enhanced Raman Scattering (SERS). *Nano Lett.* **2020**, *20*, 7655–7661. [[CrossRef](#)]
10. Xu, D.K.; Chen, H.Y. Electrochemical Detection for Arrayed Electrode Chips. *Prog. Chem.* **2009**, *21*, 2379–2387.
11. Wu, J.; Liu, H.; Chen, W.; Ma, B.; Ju, H. Device integration of electrochemical biosensors. *Nat. Rev. Bioeng.* **2023**, *1*, 346–360. [[CrossRef](#)] [[PubMed](#)]
12. Chen, Y.H.; Gao, X.L.; Liu, G.S.; Zhu, R.T.; Yang, W.L.; Li, Z.S.; Liu, F.M.; Zhou, K.C.; Yu, Z.M.; Wei, Q.P.; et al. Correlation of the role of boron concentration on the microstructure and electrochemical properties of diamond electrodes. *Funct. Diam.* **2022**, *1*, 197–204. [[CrossRef](#)]
13. Dong, X.Y.; Zhao, W.W.; Sun, G.B.; Xu, J.J.; Chen, H.Y. An Electrochemical DNA Biosensor Based on Gold Nanofilm and Stable Y Junction Structure. *Acta Chim. Sin.* **2012**, *70*, 1457–1463. [[CrossRef](#)]
14. Tong, P.; Zhang, L.; Xu, J.J.; Chen, H.Y. Simply amplified electrochemical aptasensor of Ochratoxin A based on exonuclease-catalyzed target recycling. *Biosens. Bioelectron.* **2011**, *29*, 97–101. [[CrossRef](#)]
15. Du, D.; Ju, H.X.; Zhang, X.J.; Chen, J.; Cai, J.; Chen, H.Y. Electrochemical immunoassay of membrane P-glycoprotein by immobilization of cells on gold nanoparticles modified on a methoxysilyl-terminated butyrylchitosan matrix. *Biochemistry* **2005**, *44*, 11539–11545. [[CrossRef](#)] [[PubMed](#)]
16. Luo, C.H.; Lei, Y.N.; Yan, L.; Yu, T.X.; Li, Q.; Zhang, D.C.; Ding, S.J.; Ju, H.X. A Rapid and Sensitive Aptamer-Based Electrochemical Biosensor for Direct Detection of *Escherichia coli* O111. *Electroanalysis* **2012**, *24*, 1186–1191. [[CrossRef](#)]
17. Guner, A.; Cevik, E.; Senel, M.; Alpsoy, L. An electrochemical immunosensor for sensitive detection of *Escherichia coli* O157:H7 by using chitosan, MWCNT, polypyrrole with gold nanoparticles hybrid sensing platform. *Food Chem.* **2017**, *229*, 358–365. [[CrossRef](#)]
18. Zou, Y.J.; Liang, J.; She, Z.; Kraatz, H.B. Gold nanoparticles-based multifunctional nanoconjugates for highly sensitive and enzyme-free detection of *E. coli* K12. *Talanta* **2019**, *193*, 15–22. [[CrossRef](#)] [[PubMed](#)]
19. Li, C.; Liu, C.J.; Liu, R.; Wang, Y.X.; Li, A.Y.; Tian, S.; Cheng, W.; Ding, S.J.; Li, W.T.; Zhao, M.; et al. A novel CRISPR/Cas14a-based electrochemical biosensor for ultrasensitive detection of *Burkholderia pseudomallei* with PtPd@PCN-224 nanoenzymes for signal amplification. *Biosens. Bioelectron.* **2023**, *225*, 115098. [[CrossRef](#)]
20. Li, L.L.; Yu, S.Q.; Wu, J.; Ju, H.X. Regulation of Target-activated CRISPR/Cas12a on Surface Binding of Polymer Dots for Sensitive Electrochemiluminescence DNA Analysis. *Anal. Chem.* **2023**, *95*, 7396–7402. [[CrossRef](#)]
21. Zhang, J.L.; Liu, W.J.; Li, J.H.; Lu, K.Q.; Wen, H.R.; Ren, J.L. Rapid bacteria electrochemical sensor based on cascade amplification of 3D DNA walking machine and toehold-mediated strand displacement. *Talanta* **2022**, *249*, 123646. [[CrossRef](#)] [[PubMed](#)]
22. Kwon, J.; Kang, H.Y.; Yang, H. Permeabilization-free beta-galactosidase-induction-based electrochemical detection of *Escherichia coli*. *Sens. Actuators B Chem.* **2021**, *337*, 129768. [[CrossRef](#)]
23. Ertl, P.; Mikkelsen, S.R. Electrochemical biosensor array for the identification of microorganisms based on lectin-lipopolysaccharide recognition. *Anal. Chem.* **2001**, *73*, 4241–4248. [[CrossRef](#)]
24. Johnson, B.J.; Delehanty, J.B.; Lin, B.; Ligler, F.S. Immobilized proanthocyanidins for the capture of bacterial lipopolysaccharides. *Anal. Chem.* **2008**, *80*, 2113–2117. [[CrossRef](#)]
25. Castle, L.M.; Schuh, D.A.; Reynolds, E.E.; Furst, A.L. Electrochemical Sensors to Detect Bacterial Foodborne Pathogens. *ACS Sens.* **2021**, *6*, 1717–1730. [[CrossRef](#)]
26. Myers, J.A.; Curtis, B.S.; Curtis, W.R. Improving accuracy of cell and chromophore concentration measurements using optical density. *BMC Biophys.* **2013**, *6*, 4. [[CrossRef](#)] [[PubMed](#)]
27. Beal, J.; Farny, N.G.; Haddock-Angelli, T.; Selvarajah, V.; Baldwin, G.S.; Buckley-Taylor, R.; Gershater, M.; Kiga, D.; Marken, J.; Sanchania, V.; et al. Robust estimation of bacterial cell count from optical density. *Commun. Biol.* **2020**, *3*, 512. [[CrossRef](#)]
28. Wos, M.L.; Pollard, P.C. Cellular nicotinamide adenine dinucleotide (NADH) as an indicator of bacterial metabolic activity dynamics in activated sludge. *Water Sci. Technol.* **2009**, *60*, 783–791. [[CrossRef](#)]
29. Mao, X.Y.; Wu, Y.H.; Xu, L.L.; Cao, X.J.; Cui, X.J.; Zhu, L.D. Electrochemical biosensors based on redox carbon nanotubes prepared by noncovalent functionalization with 1,10-phenanthroline-5,6-dione. *Analyst* **2011**, *136*, 293–298. [[CrossRef](#)]

30. Dube, I.; Jimenez, D.; Fedorov, G.; Boyd, A.; Gayduchenko, I.; Paranjape, M.; Barbara, P. Understanding the electrical response and sensing mechanism of carbon-nanotube-based gas sensors. *Carbon* **2015**, *87*, 330–337. [[CrossRef](#)]
31. Wang, T.T.; Zhao, D.L.; Guo, X.F.; Correa, J.; Riehl, B.L.; Heineman, W.R. Carbon Nanotube-Loaded Nafion Film Electrochemical Sensor for Metal Ions: Europium. *Anal. Chem.* **2014**, *86*, 4354–4361. [[CrossRef](#)] [[PubMed](#)]
32. Chen, Y.F.; Wang, D.C.; Liu, Y.R.; Gao, G.Y.; Zhi, J.F. Redox activity of single bacteria revealed by electrochemical collision technique. *Biosens. Bioelectron.* **2021**, *176*, 112914. [[CrossRef](#)] [[PubMed](#)]
33. Ge, B.; Tan, Y.; Xie, Q.; Ma, M.; Yao, S. Preparation of chitosan–dopamine-multiwalled carbon nanotubes nanocomposite for electrocatalytic oxidation and sensitive electroanalysis of NADH. *Sens. Actuators B Chem.* **2009**, *137*, 547–554. [[CrossRef](#)]
34. Liu, A.; Watanabe, T.; Honma, I.; Wang, J.; Zhou, H. Effect of solution pH and ionic strength on the stability of poly(acrylic acid)-encapsulated multiwalled carbon nanotubes aqueous dispersion and its application for NADH sensor. *Biosens. Bioelectron.* **2006**, *22*, 694–699. [[CrossRef](#)]
35. Li, Z.; Huang, Y.; Chen, L.; Qin, X.; Huang, Z.; Zhou, Y.; Meng, Y.; Li, J.; Huang, S.; Liu, Y.; et al. Amperometric biosensor for NADH and ethanol based on electroreduced graphene oxide–polythionine nanocomposite film. *Sens. Actuators B Chem.* **2013**, *181*, 280–287. [[CrossRef](#)]
36. Zhai, X.; Wei, W.; Zeng, J.; Gong, S.; Yin, J. Layer-by-Layer Assembled Film Based on Chitosan/Carbon Nanotubes, and its Application to Electrocatalytic Oxidation of NADH. *Microchim. Acta* **2006**, *154*, 315–320. [[CrossRef](#)]
37. Sangamithirai, D.; Narayanan, V.; Muthuraaman, B.; Stephen, A. Investigations on the performance of poly(o-anisidine)/graphene nanocomposites for the electrochemical detection of NADH. *Mater. Sci. Eng. C* **2015**, *55*, 579–591. [[CrossRef](#)]
38. Arthisree, D.; Devi, K.S.S.; Devi, S.L.; Meera, K.; Joshi, G.M.; Senthil Kumar, A. A hydrophobic coenzyme Q10 stabilized functionalized-MWCNT modified electrode as an efficient functional biomimetic system for the electron-transfer study. *Colloids Surf. A Physicochem. Eng. Asp.* **2016**, *504*, 53–61. [[CrossRef](#)]
39. Eguílaz, M.; Gutiérrez, A.; Rivas, G. Non-covalent functionalization of multi-walled carbon nanotubes with cytochrome c: Enhanced direct electron transfer and analytical applications. *Sens. Actuators B Chem.* **2016**, *225*, 74–80. [[CrossRef](#)]

Disclaimer/Publisher’s Note: The statements, opinions and data contained in all publications are solely those of the individual author(s) and contributor(s) and not of MDPI and/or the editor(s). MDPI and/or the editor(s) disclaim responsibility for any injury to people or property resulting from any ideas, methods, instructions or products referred to in the content.